INSTITUTE OF PHYSICS PUBLISHING JOURNAL OF PHYSICS B: ATOMIC, MOLECULAR AND OPTICAL PHYSICS

J. Phys. B: At. Mol. Opt. Phys. **35** (2002) 4211–4221 PII: S0953-4075(02)35843-7

Electron scattering and ionization of ozone, O_2 and O_4 molecules

K N Joshipura[1], B K Antony[1] and Minaxi Vinodkumar[1,2]

[1] Department of Physics, Sardar Patel University, Vallabh Vidyanagar-388 120, India
[2] VP & RPTP Science College, Vallabh Vidyanagar-388 120, India

Received 11 April 2002, in final form 16 August 2002
Published 8 October 2002
Online at stacks.iop.org/JPhysB/35/4211

Abstract

Total cross sections (TCSs) including ionization cross sections for the impact of intermediate and high energy electrons on ozone as well as O, O_2 and O_4 targets are calculated and compared with available measurements. The calculation proceeds through a complex energy-dependent potential derived from the atomic/molecular electron charge density. The summed total inelastic cross sections determined in this formalism are used to derive *total ionization cross sections* Q_{ion}, as done in our recent work on many other atomic and molecular targets. The present TCS results show good accord with the recent experimental data on e–O_3 scattering, but the corresponding ionization results favour the available theoretical rather than the experimental data. Our results on atomic and molecular oxygen show good accord with previous investigations of other workers. Preliminary estimates on O_4 are also given.

(Some figures in this article are in colour only in the electronic version)

1. Introduction

This paper reports our theoretical studies on electron scattering and ionization of ozone together with atomic and molecular oxygen and a lesser known target O_4, which may be called an $(O_2)_2$ dimer. Electron scattering from most of the atmospheric atoms and molecules has been investigated well for a long time [1]. The interest in the ozone target is of recent origin [2], in view of its importance in the terrestrial uv radiation budget. On the experimental front, the total electron scattering cross sections for O_3 are available now with the recent work of Pablos *et al* [3] in the energy range 350–5000 eV. The total *ionization* cross sections (Q_{ion}) of electron collisions on ozone molecules were measured some years ago by Seigel [4] and by Newson *et al* [5]. The aim of the present paper is thus threefold. We aim to provide here the calculated data for comparison with the recent measurements of total electron scattering cross sections for molecular ozone. The calculation we report here is carried out within the framework of the complex potential comprising well known model potential terms. Employing a simple method we extend these calculations to obtain total *ionization* cross sections for comparisons

against the available data. We also wish to make a comparative study of the total cross sections (TCSs) of the oxygen species O–O_2–O_3–O_4, determined within a common general formalism. Total as well as ionization cross sections of electron scattering considered in this paper find relevance in a variety of pure and applied fields these days. In particular, the TCS of e–O_3 collisions are important in modelling the energy deposition in the upper atmospheres of the Earth and other planets [3].

Since ozone is a weakly polar molecule ($D = 0.21$ au nearly), the long range dipole potential becomes a small perturbation over short range interactions as energy increases. Therefore, the electron impact dipole rotation gives a very small contribution [1] to the overall total cross section in the present range of intermediate and high energies $E_i = 20$–2000 eV. Our calculations in this paper are based on electron–molecule collision dynamics in the form of a spherical energy-dependent complex potential, $V_{opt} = V_R + \mathrm{i}V_I$. We employ this in the Schrödinger equation to calculate the relevant cross sections. The imaginary term V_I, also called the absorption potential V_{abs}, accounts for all energetically allowed inelastic *electronic* channels including ionization.

Amongst the earlier theories on electron–atom/molecule ionization, mention must be made of the Born–Bethe approximation, as discussed by Inokuti [6]. This approximation starts with the Born inelastic cross sections and arrives at the high energy ionization cross sections. Kim and co-workers [7] and also Khare and associates [8] have extended the use of this approximation by combining, in different ways, the terms describing 'hard' or near-by collisions and 'soft' or distant collisions. Our present theoretical approach starts with the following observation. Although the open electronic channels include transitions to discrete states as well as the continuum, the ionization becomes the dominant process as E_i increases above the threshold. Hence the summed total inelastic cross section Q_{inel} resulting from the partial wave analysis of V_{abs} can be effectively used to deduce the ionization contribution. We have successfully employed this approach to a number of atomic and molecular targets. A preliminary version [9] of this approach was used to obtain the Q_{ion} of the radicals CH_x, NH_x ($x = 1$–3) and OH *vis-à-vis* their parent molecules. An improved calculation has been reported by us recently on Ne and Ne* atoms [10] as well as on atomic and molecular halogens [11]. Details of the input model potentials needed for constructing the V_{opt} may be found in our earlier papers [12, 13].

The main quantities calculated in the present paper are the total (complete) cross section (TCS) Q_T, the total *elastic* cross section Q_{el}, the summed total *inelastic* cross section Q_{inel} and the total *ionization* cross section Q_{ion}. The first three of these quantities are such that

$$Q_T(E_i) = Q_{el}(E_i) + Q_{inel}(E_i). \tag{1}$$

The first term Q_{el} represents an electronically as well as vibrationally elastic total cross section.

In fact the present calculations are vibrationally unresolved in view of our range of incident energy [1]. Now, for polar molecules the nonspherical part of the e–molecule interaction is dominated by the dipole potential. Let us also define the *grand total cross section* denoted by Q_{TOT}, representing spherical as well as non-spherical (dipole) e–molecule interactions, as follows:

$$Q_{TOT}(E_i) = Q_T(E_i) + Q_{rot}(E_i) \tag{2}$$

where on the RHS the second term Q_{rot} denotes the TCS of the dipole rotational excitation. This term, required presently for the O_3 target only, is obtained adequately in the first Born approximation [14]. The point-dipole first Born approximation is justified here [15, 16], since the target is only weakly polar, and the energies of our interest are typically above 20 eV or so.

This paper employs well defined potentials and well known theoretical methods to the extent of calculating the quantities of equations (1) and (2). Now, since the inelastic electronic

channels consist of discrete excitations and ionizations, we can express the second term of equation (1) as follows:

$$Q_{inel}(E_i) = \sum Q_{exc}(E_i) + Q_{ion}(E_i). \tag{3}$$

In this break-down, the first term is the sum over total *excitation* cross sections for all accessible electronic transitions, while the second term indicates the total cross section of all allowed ionization processes of the target by the incident electrons. The first term arises mainly from the low lying dipole allowed transitions for which the cross sections become small progressively above the ionization threshold. Hence, as the incident energy increases the second term in equation (3) dominates over the first, so that the calculated inelastic quantity Q_{inel} can be employed to derive the total ionization cross section Q_{ion}. This theoretical approach, to be called the 'complex scattering potential–ionization contribution' or CSP–ic method, is highlighted in section 2. It explores the advantages of the well known complex-potential representation of simultaneous elastic and inelastic scattering, above the ionization threshold.

2. Theory

The present (CSP–ic) approach rests on the spherical energy-dependent complex potential derived from the electronic charge density of the target atom [17] or the molecule [13] of our interest. For the O_2 and O_3 molecules an average spherical charge density $\rho(r)$ is generated by expanding the atomic charge densities at the molecular centre of mass. In the single-centre expansion of the molecular charge density the spherical term is dominant, hence the use of spherical potentials is justified. The relatively weaker anisotropy in this charge distribution gives rise to rotational inelasticity, as included approximately in equation (2). The charge density $\rho(r)$ is corrected to comply with an appropriate asymptotic form as a function of the molecular ionization energy I [18]. The said correction accounts for the distortion of the valence electron charge density in the formation of covalent bonding. The single-centre molecular potential generated from this charge density has a real part V_R, which consists of static (V_{st}), exchange (V_{ex}) and polarization (V_{pol}) terms. These potential terms for each target are obtained from the $\rho(r)$ and other relevant atomic or molecular properties.

Next, the imaginary potential term V_{abs} is considered in the well known quasi-free Pauli-blocking model of Staszewska *et al* [19], after some modification discussed below. This is an energy-dependent potential that accounts for all possible electronic inelastic channels cumulatively, and has the generic form, in atomic units,

$$\begin{aligned} V_{abs}(r, E_i) &= -\tfrac{1}{2}\rho(r)v_{loc}\sigma_{ee} \\ &= -\rho(r)\left(\frac{T_{loc}}{2}\right)^{1/2}\left(\frac{8\pi}{10k_F^3 E_i}\right)\theta(p^2 - k_F^2 - 2\Delta)(A_1 + A_2 + A_3). \end{aligned} \tag{4}$$

In the above expressions v_{loc} is the local speed of the external electron, and σ_{ee} denotes the average cross section of the binary collision of the external electron with one of the target electrons. The local kinetic energy of the external electron is obtained from

$$T_{loc} = E_i - V_R = E_i - (V_{st} + V_{ex}) \tag{5}$$

where we have excluded the relatively insignificant polarization term V_{pol}.

In equation (4), $p^2 = 2E_i$, k_F is the Fermi wavevector and Δ is an energy parameter. Further, $\theta(x)$ is the Heaviside step-function, such that $\theta(x) = 1$ for $x > 0$, and is zero otherwise. The dynamic functions A_1, A_2 and A_3, which are given in Staszewska *et al* [19], depend differently on $\rho(r)$, I, Δ and E_i. The parameter Δ, assumed to be fixed in the original model, determines a threshold below which $V_{abs} = 0$, and the ionization or excitation

is prevented energetically. Now, our modification here is to choose the value of Δ by the following consideration. At energy of impact close to the (vertical) ionization threshold I, the excitations to the discrete states also take place, but as E_i increases the valence ionization becomes dominant, together with the possibility of ionization of the inner electronic shells. In the range of intermediate energies the V_{abs} shows a rather excessive loss of flux into the inelastic channels. The potential also penetrates in the region of inner electronic shells, which are of course harder to excite or ionize. In order to rectify the said behaviour of this potential, we choose $\Delta \approx I$ for low E_i and $\Delta > I$ at E_i near the position of the peak of Q_{inel}. Thus, our modification is to express Δ as a slowly varying function of E_i around I. For nearly all the targets investigated by us so far [9–11], this choice of Δ results in a better agreement of our calculations with the compared data. The next step is to solve the Schrödinger equation with the modified V_{abs}, using the appropriate boundary conditions. This yields the imaginary part of the phase shifts Im $\delta_l(k)$ for various partial waves l. We have omitted here the standard formulae [20] used to generate Q_{inel} as well as the Q_{el} by employing the real and the imaginary parts of $\delta_l(k)$. The TCS Q_T is given by equation (1).

The inelastic cross section Q_{inel} is not accessible directly in experiments, but since that quantity itself is partitioned according to equation (3), it follows that

$$Q_{inel}(E_i) \geqslant Q_{ion}(E_i). \tag{6}$$

At incident energies above I, the ionization plays a dominant role here due to the availability of infinitely many open channels of scattering. In order to determine Q_{ion} from the calculated Q_{inel}, let us introduce the following quantity for a given target:

$$R(E_i) = \frac{Q_{ion}(E_i)}{Q_{inel}(E_i)} \tag{7}$$

such that

$$0 \leqslant R \lesssim 1.$$

For a number of stable molecules like H_2, O_2, H_2O, CH_4 etc, the threshold of valence ionization lies roughly within 10–15 eV, and the thresholds for the low lying electronic excitations are under 10 eV or so. For these targets the experimental ionization cross sections Q_{ion} are known accurately, and it is observed [1, 9–11] that

$$R(E_i) \cong 0.7, \qquad \text{up to } E_i \cong E_p \tag{8a}$$

$$\cong 1, \qquad \text{for } E_i > E_p \tag{8b}$$

where E_p stands for the incident energy at which the calculated Q_{inel} attains its maximum.

Actually the ratio R as in equation (8a) may be slightly different for different targets, but the representative value given here is based on a general trend, and it serves as an input for further work. Next, we represent this ratio as a continuous function of energy ($E_i \geqslant I$) in the following manner:

$$R(E_i) = 1 - C_1\left[\frac{\ln(U)}{U} + \frac{C_2}{U+a}\right]. \tag{9}$$

Here U is the dimensionless variable defined as

$$U = \frac{E_i}{I}. \tag{10}$$

Thus, $R(E_i)$ approaches unity at high energies when the dipole allowed electronic excitations fall off as $\ln E_i/E_i$. The second term in the square bracket in equation (9) ensures a better energy dependence at low and intermediate E_i. To determine the dimensionless parameters C_1, C_2 and a appearing in equation (9), we note the following three general conditions on the ratio R:

(i) it is zero at and below the ionization threshold,
(ii) it behaves in accordance with equation (8*a*) at the peak position E_p and
(iii) it approaches 1 asymptotically for E_i sufficiently larger than E_p.

The present expression for R, i.e. equation (9), differs slightly from that of our previous work [10, 11]. The equations (7)–(10) define the present CSP–ic method.

Rigorous calculation of the quantity R in particular and the cross section Q_{ion} in general, for an atom or a molecule, poses a very difficult problem. As regards the ionization calculations, various semi-quantal theories are in vogue in the current literature. Two of the fairly well known approaches, namely the binary encounter dipole (BED) and binary encounter Bethe (BEB) models of Kim *et al* [7] as well as the Deutsch–Maerk (DM) formalism [21], seek to calculate the electronic shell-wise contribution to the molecular Q_{ion} under different approximations. A very simple procedure, called the 'defect concept' or the DC method [22], expresses the molecular Q_{ion} of a diatomic target X_2 in terms of the constituent atom cross section $Q_{ion}(X)$, as follows:

$$Q_{ion}(X_2) = 2^{\beta} Q_{ion}(X) \tag{11}$$

with

$$\beta = 1 - \gamma. \tag{12}$$

The value $\gamma \approx 0.2$ as chosen by Deutsch *et al* [22] arises from the fact that a molecule is not a *simple* combination of atoms. This calculation [22] can give reasonable molecular cross sections at intermediate energies, where interference effects, due to the two-centre nature of the target, are important. At high energies, where the independent atom model (IAM) for electron–molecule scattering holds, a simple 'additivity rule' (i.e. $\beta = 1$) is still reliable [3, 12].

3. Results, discussion and conclusions

In light of our formulation discussed above we have examined the collisions of medium to high energy electrons incident on ozone, and have also calculated and compared the electron scattering properties of the O–O_2–O_3–O_4 targets. The results of our calculations for the TCS Q_{TOT}, Q_T and Q_{ion} for these systems are highlighted in figures 1–5 and in tables 1 and 2. Not shown here are the calculated values of the cross section Q_{inel}, although that quantity itself exhibits the broad features of Q_{ion} [9–13]. As discussed in our previous paper [9] the calculated Q_{inel} for molecules H_2O, CH_4 etc exceed Q_{ion} at the peak by about 25%, and the two cross sections tend to merge beyond 800 eV or so. The present calculations have confirmed this trend. Let us also mention briefly the two choices for the energy parameter Δ employed in the potential V_{abs}. In the case of O_2 when the energy is 100 eV, we have $Q_{inel} = 4.10$ Å^2 with $\Delta = I$, as against the value 3.74 Å^2 with Δ varying slowly as $\ln E_i/E_i$ around I. The two cross section values differ by about 9%. Generally the Q_{inel} predicted with $\Delta = I$ are found to be on the higher side. Therefore the choice for Δ as a variable around I is more suitable for the present work.

Let us examine briefly the quantity R required to determine the Q_{ion} in the CSP–ic method, as obtained from equation (9). The behaviour of this ratio as a function of energy above the ionization threshold is plotted in figure 1 for three typical targets, namely the Ne atom ($I = 21.64$ eV), O_2 ($I = 12.07$ eV) and CH_4 ($I = 12.61$ eV). Table 1 gives the target properties and the parameters employed to obtain $R(E_i)$ from equations (9) and (10). The difference in the variation of R for different targets as seen from figure 1 depends mainly on the ionization threshold I, and to a small extent on the peak position E_p (see equation (8)).

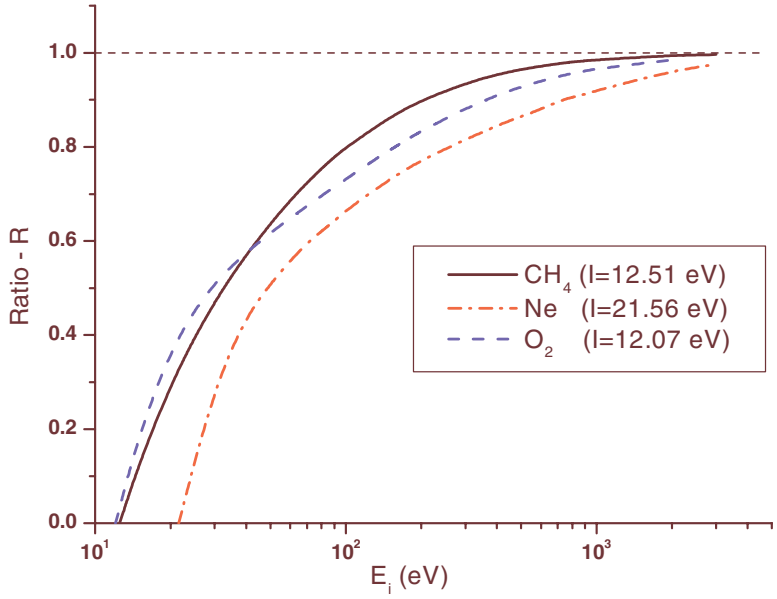

Figure 1. The ratio R as a function of E_i, for O_2, Ne and CH_4 targets.

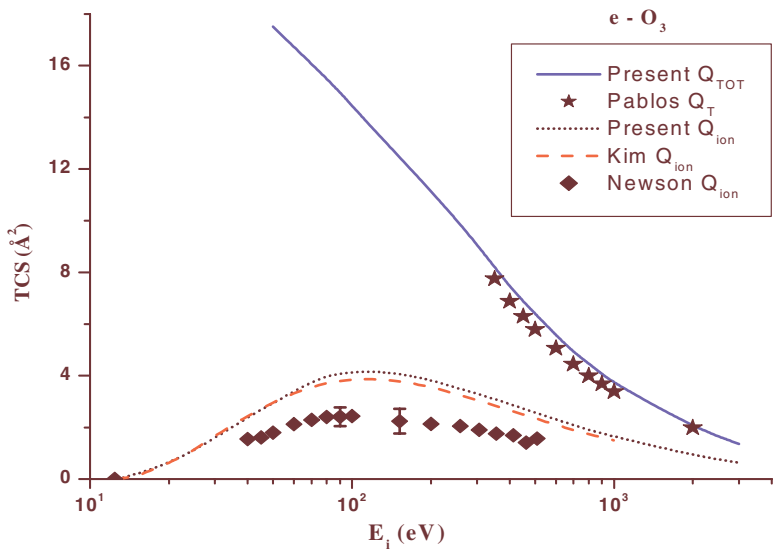

Figure 2. e–O_3 collisions: ——, Q_{TOT} (this paper); ★★★, exp Q_T [3]; · · · · · ·, Q_{ion} (this paper); - - - -, Q_{ion} BEB [7]; ◆◆◆, exp Q_{ion} [5].

In the present range of energy (20–2000 eV), it is the single rather than multiple ionization that contributes most to Q_{ion}. Let us also note that while comparing our calculated molecular Q_{ion} with the experiments, we have combined the parent and the dissociative ionization cross sections, as reported in the measured data-sets.

Now, consider first the various TCSs of e–O_3 collisions. Figure 2 shows our results on Q_{TOT} and Q_{ion} against the available experimental data. The dipole rotation (see equation (2))

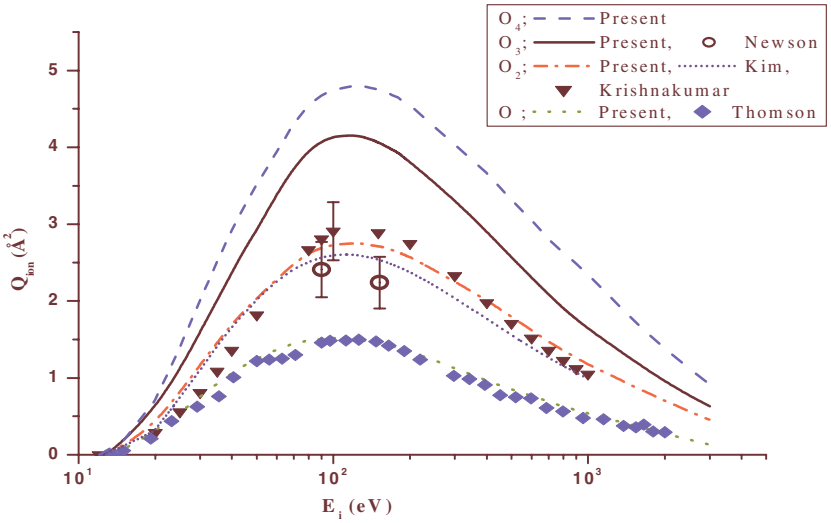

Figure 3. Ionization cross sections of O, O_2, O_3 and O_4 (from bottom to top). O atoms: - - - -, this paper; ♦♦♦, exp Q_{ion} [23]. O_2 molecules: — · —, Q_{ion} (this paper); · · · · · ·, Q_{ion} BEB [7]; ▼▼▼, exp Q_{ion} [25]. O_3 molecules: ——, Q_{ion} (this paper); ○○○, exp Q_{ion} [5]. $(O_2)_2$ dimer or O_4 molecules: – – –, Q_{ion} (this paper).

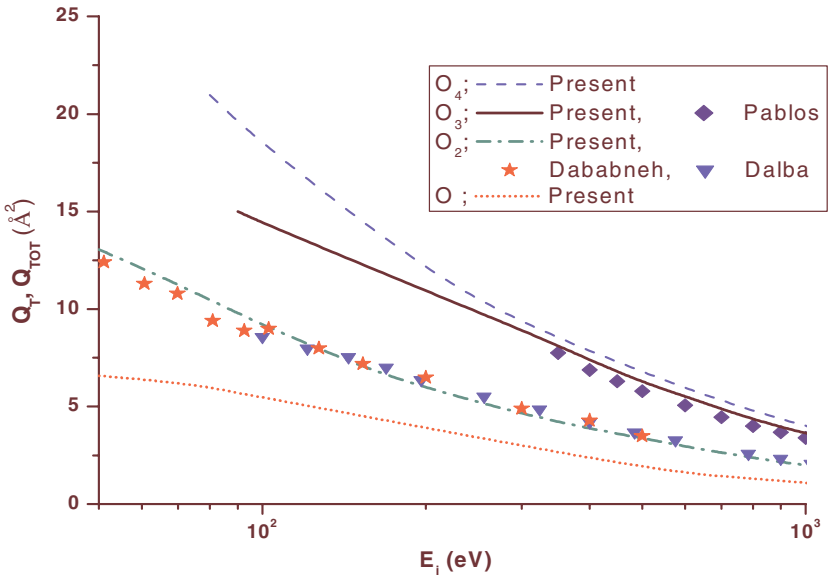

Figure 4. The total (complete) cross section Q_T for O, O_2, O_3 and O_4 (from bottom to top). O atoms: · · · · · ·, Q_T (this paper). O_2 molecules: — · —, this paper; ★★★, exp [29]; ▼▼▼, exp [28]. O_3 molecules: ——, this paper; ♦♦♦, exp [3]. $(O_2)_2$ dimers: – – –, this paper.

has very little effect in Q_{TOT} at the energies of our interest. The TCSs with and without the dipole contribution (not shown separately) merge after 200 eV. The present TCSs Q_{TOT} (see the upper curve in figure 2) are in excellent agreement with the measurements of Pablos *et al* [3], and are well within the experimental error of about 10% at all energies. The present

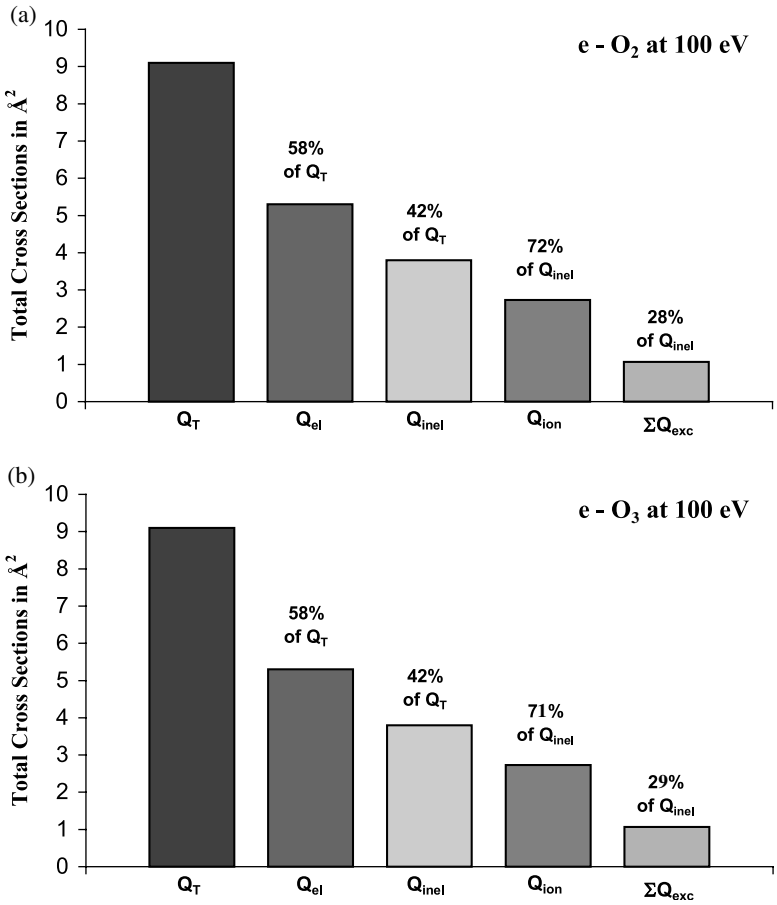

Figure 5. (a) Relative contributions of various TCSs in e–O_2 collisions at 100 eV; (b) the same as in (a) but for e–O_3 collisions

Table 1. Ionization energies (*CRC Handbook*, [30]) and other target parameters used in this work.

Target	I (eV)	E_p (eV)	C_1	C_2	a
O atom	13.60	100	−1.204	−7.859	8.461
O_2	12.07	120	−1.073	−7.631	7.191
O_3	12.43	120	−1.151	−10.267	10.820
Ne	21.56	150	−1.064	−8.614	8.164

theoretical work also provides useful data on Q_{TOT} below 350 eV, where experimental or other values are not available.

The lower curves for ozone in figure 2 compare our theoretical Q_{ion} with the experimental data of Newson *et al* [5]. These data were normalized relative to the earlier measurements made by Seigel [4], which were limited to 100 eV energy. The data of [4] are not shown here. As the figure shows, the present CSP–ic calculations on Q_{ion} agree with the BEB model of Kim *et al* [7], but both these theoretical results are higher than the measurements on ozone [4, 5]. The disagreement in the peak region is far more than the 15% error margin of the measured data. As noted by Deutsch *et al* [21] the results of the DM formalism for Q_{ion} also differ

Table 2. The present total (complete) and ionization cross sections (in $Å^2$) of oxygen systems.

	O atom		O_2 molecule		O_3 molecule		$(O_2)_2$ dimer	
Energy (eV)	Q_T	Q_{ion}	Q_T	Q_{ion}	Q_{TOT}	Q_{ion}	Q_T	Q_{ion}
20	7.29	0.30	—	0.42	—	0.62	—	0.73
30	7.07	0.76	—	1.17	—	1.60	—	2.04
50	6.57	1.25	13.04	2.04	17.81	2.92	26.08	3.55
80	5.87	1.49	10.48	2.62	15.69	3.96	20.96	4.55
100	5.41	1.54	9.21	2.73	14.58	4.14	18.42	4.75
200	3.85	1.35	5.96	2.57	11.25	3.81	11.92	4.55
300	3.00	1.13	4.63	2.25	9.02	3.31	9.26	4.04
500	1.95	0.85	3.38	1.79	6.29	2.57	6.76	3.32
700	1.42	0.69	2.64	1.47	4.94	2.08	5.28	2.80
1000	1.02	0.54	1.98	1.17	3.67	1.64	3.96	2.34
1500	0.65	0.38	1.41	0.88	2.65	1.19	2.82	1.76
2000	0.46	0.28	1.08	0.69	2.02	0.92	2.16	1.38

from these measurements [5] in a similar way. The present and the BEB values (figure 2) are nearly merging in the low as well as high energy limits. In the peak region at about 100 eV, our calculations indicate that the Q_{ion} of O_3 are about 30% of its Q_{TOT}. For atomic and molecular oxygen targets also the maximum ionization contribution to their Q_T is similar.

Now figure 3 reveals further details of the present and the previous total ionization cross sections for all the *four* targets investigated in this study. Consider first the lowest curve in this figure. It represents our Q_{ion} for *atomic* oxygen determined in the CSP–ic method. The present values are in very good accord with the experimental data given by Thomson *et al* of the Belfast group [23] at all energies. In the region of the maximum the present values for O atoms are also similar to the calculated data of Margreiter *et al* [24], not plotted here. Further, the present calculations on the Q_{ion} for O_2 molecule also find good accord with the measurements of Krishnakumar and Srivastava [25], within their 10% error margin. We have not included several other experimental data on molecular oxygen, since the conclusions are similar. Besides this, as figure 3 shows, there is also a fair agreement between the present values and the BEB [7] cross sections for ionization of the O_2 molecule.

Also shown here for comparison are the present total ionization cross sections of O_3. These are larger than those of O_2, and we find from our results that at the peak position near 100 eV

$$\frac{Q_{ion}(O_3)}{Q_{ion}(O_2)} = 1.52.$$

The above value is quite close to the ratio 1.5 of the respective total number of electrons. However, one notes here again that the measured data on ozone [4, 5] are rather *lower* and they actually lie very much in the range of all the O_2 results.

The present investigation includes (see figures 3 and 4) our study on the electron scattering and ionization of the *dimer* $(O_2)_2$, about which nothing much is known at present. The motivation for this study comes from the fact that dimers and clusters are exotic forms of matter, and that their investigation requires electron impact cross sections including those of ionization. Theoretical studies on the structures of loosely bound Van der Waals dimers such as $(O_2)_2$ have been made in [26]. The O_4 molecule, regarded as the dimer of O_2 with parallel coplanar D_{2h} geometry, exhibits a rather large intermolecular separation of about $6\,a_0$, as against the 'monomer' bond length $R_{O–O} = 2.29\,a_0$. We have extended our present calculations to cover the $(O_2)_2$ target through the application of the DC method (equations (11) and (12)) by

considering the O_2 molecule as the constituent unit (i.e. X in equation (11)) in this dimer. This approach is justified since the 'independent *scatterer* approximation' [12, 27] holds better here, in view of the large intermolecular separation and a rather low binding energy of the $(O_2)_2$ system. However as noted recently by us [11], a constant value $\beta = 0.8$ in equations (11), (12) underestimates the Q_{ion} towards high energies. Therefore in the present work the index β is allowed to increase linearly from 0.8 up to the peak of Q_{ion} to unity at higher values of energy. Preliminary estimates on the electron-induced Q_{ion} of this dimer made in this way are exhibited by the top curve in figure 3. All the present total ionization cross sections given in this figure are consistent with the respective target properties of the oxygen species, namely ionization threshold, the bond lengths and the total number of target electrons.

We have given in figure 4 a common plot of the total (*complete*) cross sections Q_T of the targets O, O_2, O_4 and Q_{TOT} of the molecule O_3. The lowest curve here corresponds to atomic oxygen. This figure indicates a very good agreement of the present Q_T values with the previous experimental data on the O_2 molecule, obtained some years ago by two different groups [28, 29]. At high energies the TCSs of O, O_2 and O_3 are in keeping with their polarizabilities and their total number of electrons. The present CSP–ic method has been employed in the O, O_2 and O_3 cases, but the $(O_2)_2$ target requires a further approximation as follows. Within the independent scatterer approximation [12, 27], we assume the TCS Q_T of $(O_2)_2$ to be twice that of O_2.This corresponds to $\beta = 1$ in equation (11). This approximation holds better for a dimer, rather than for a diatomic molecule, as explained above. The TCSs of the dimer derived in this way in figure 4 show an upper limit of the Q_T for $(O_2)_2$. The lower limit in this case would of course be given by the corresponding O_3 results.

The bar-charts presented in figures 5(a) and (b), corresponding to O_2 and O_3 respectively, exhibit the relative contributions of various TCSs to the total (complete) cross section of electron collisions at 100 eV. At this energy when the Q_{ion} is almost maximum, the distribution between ionization and electronic excitations can also be seen from these figures. The information (see figures 5(a) and (b)) derived from the present calculations gives an approximate but overall theoretical picture of the above-threshold processes of electron scattering in these targets. This will be useful in view of existing discrepancies in the sum checks of various TCS, obtained from independent theories or experiments.

Finally, our table 2 gives the numerical values of the present TCS for the sequence O–O_2–O_3–O_4.

In conclusion, this paper reports the different TCSs of electron scattering on oxygen and ozone molecules, together with O and O_4 targets, above the ionization threshold up to about 2000 eV. The total (complete) cross sections calculated here in a complex scattering potential approach support the earlier measured data on O_2 and the recent experimental results on ozone [3] very well. The total *ionization* cross sections of ozone obtained here by us favour the earlier two theories, namely the BEB model and the DM formalism, as against the available experimental data [4, 5]. Since the present method seeks to extract the ionization contribution from the total inelastic cross sections, our theoretical Q_{ion} tend to be on the higher side of the other theoretical and experimental data. However, this fact alone does not explain the large discrepancy between the present theory and the experiments [4, 5] for ozone. Therefore, a fresh measurement of absolute total ionization cross sections of ozone is required in order to resolve the said discrepancy. In general there is a need for a rigorous theory on electron–atom/molecule ionization, since the present and the previous theories mentioned in this work are semiempirical.

The theoretical approach adopted in this paper yields consistent results for O, O_2 and O_3. The new results on Q_T and Q_{ion} reported here for the relatively unknown $(O_2)_2$ target are expected to be reliable.

Acknowledgments

The authors thank the Department of Science and Technology (New Delhi, India) for a research grant under which this work was mainly carried out.

KNJ is thankful to the Royal Society of London, UK as well as the Indian National Science Academy, New Delhi, India for his visit to the Department Of Physics and Astronomy, University College London, UK under a bilateral collaboration programme, during which part of the above work was carried out. We (KNJ and MV) also acknowledge with many thanks the discussions with Dr Nigel Mason, Molecular Physics Laboratory, Department of Physics and Astronomy, UCL, UK.

References

[1] Jain A and Baluja K L 1992 *Phys. Rev.* A **45** 202
See also
Karwasz G P, Brusa R S and Zecca A 2001 *Rev. Nuovo Cimento* **24** 1
[2] Rees M H 1989 *Physics and Chemistry of the Upper Atmosphere* (Cambridge: Cambridge University Press)
[3] Pablos de J L, Tegeder P, Williart A, Blanco F, Garcia G and Mason N J 2002 *J. Phys. B: At. Mol. Opt. Phys.* **35** 865
[4] Seigel M W 1982 *Int. J. Mass Spectrom. Ion Process.* **44** 19
[5] Newson K A, Luc S M, Price S D and Mason N J 1995 *Int. J. Mass Spectrom. Ion Process.* **148** 203
[6] Inokuti M 1971 *Rev. Mod. Phys.* **11** 297
[7] Kim Y-K, Hwang W and Weinberger N M 1997 *J. Chem. Phys.* **106** 1026
See also their website, http://physics.nist.gov/PhysRefData/Ionization
[8] Khare S P, Sharma M K and Tomar S 1999 *J. Phys. B: At. Mol. Opt. Phys.* **32** 3147
[9] Joshipura K N and Minaxi V 2001 *J. Phys. B: At. Mol. Opt. Phys.* **34** 509
[10] Joshipura K N and Antony B K 2001 *Phys. Lett.* A **289** 323
[11] Joshipura K N and Limbachiya C G 2002 *Int. J. Mass Spectrom.* **216** 239
[12] Joshipura K N and Patel P M 1996 *J. Phys. B: At. Mol. Opt. Phys.* **29** 3925
See also
Joshipura K N and Patel P M 1994 *Z. Phys.* D **29** 269
[13] Joshipura K N and Minaxi V 1999 *Eur. Phys. J.* D **5** 229
[14] Jain A 1988 *J. Phys. B: At. Mol. Opt. Phys.* **21** 905
[15] Itikawa Y 1978 *Phys. Rep.* C **46** 117
[16] Collins L A and Norcross D W 1978 *Phys. Rev.* A **19** 116
[17] Bunge C F, Barrintos J A and Bunge A V 1993 *At. Data Nucl. Data Tables* **53** 113
[18] Patil S H 1999 *At. Data Nucl. Data Tables* **71** 41
[19] Staszewska D, Schwenke D W, Thirumalai D and Truhlar D G 1984 *Phys. Rev.* A **29** 3078
[20] Joachain C J 1983 *Quantum Collision Theory* (Amsterdam: North-Holland) p 110
[21] Deutsch H, Becker K, Matt S and Maerk T D 2000 *Int. J. Mass Spectrom.* **197** 37
[22] Deutsch H, Becker K and Maerk T D 2000 *Eur. Phys. J* D **12** 283
[23] Thompson W R, Shah M B and Gilbody H B 1995 *J. Phys. B: At. Mol. Opt. Phys.* B **28** 1321
[24] Margreiter D, Deutsch H and Maerk T D 1994 *Int. J. Mass Spectrom. Ion Process* **139** 127
[25] Krishnakumar E and Srivastava S K 1992 *Int. J. Mass Spectrom. Ion Process.* **113** 1
[26] Bussery-Honvault B and Veyret V 1998 *J. Chem. Phys.* **108** 3243
[27] Mott N F and Massey H S W 1965 *The Theory of Atomic Collisions* (Oxford: Clarendon)
[28] Dalba G, Fornasini P, Grisenti R, Ranieri G and Zecca A 1980 *J. Phys. B: At. Mol. Phys.* **13** 4695
[29] Dababneh M S, Hsieh Y-F, Kauppila W E, Kwan C K, Smith S J, Stein T S and Uddin M N 1998 *Phys. Rev.* A **38** 1207
[30] Lide D R (ed) 2000 *CRC Handbook Of Physics and Chemistry* (Boca Raton, FL: Chemical Rubber Company) pp 9–42